

Hill Restricted Three-Body Problem

Nima Fariborzi*

University of California, San Diego, La Jolla, 92093, United States of America

Michael Puso†

University of California, San Diego, La Jolla, 92093, United States of America

Christopher Lin‡

University of California, San Diego, La Jolla, 92093, United States of America

The Hill Restricted Three-Body Problem serves as a framework under which many classical analyses can be performed. In the following report, we will compute the invariant stable and unstable manifolds about the L2 equilibrium point, investigate zero-velocity curves and surfaces and trajectories in their vicinity, visualize a family of stable, periodic orbits, and finally generate the Poincaré maps and calculate the Lyapunov Characteristic Exponents to determine the stability of those periodic orbits.

I. Introduction

THE Hill restricted three-body problem is a mathematical model used to study the motion of three celestial bodies, typically a larger primary body and two smaller secondary bodies. It is named after the American astronomer George William Hill, who formulated the problem in the late 19th century. The Hill problem assumes that the two secondary bodies have significantly smaller masses compared to the primary body, and their gravitational interaction is relatively weak. The primary body is often considered as a massive central object, such as a planet or a star, while the secondary bodies are typically satellites or small celestial bodies orbiting the primary.

In this restricted three-body problem, the motion of the secondary bodies is analyzed from the perspective of a coordinate system rotating with the motion of the secondary about the primary. This rotating frame of reference simplifies the equations of motion and allows for a clearer understanding of the dynamics involved. One of the most well-known examples of the Hill restricted three-body problem is the study of the motion of a small satellite around a planet's moon. The primary force governing the satellite's motion is its gravitational attraction to the moon, while the planet is treated as a perturbation.

The Hill restricted three-body problem has various applications in astrodynamics, celestial mechanics, and space exploration. It is used to analyze the stability of satellite orbits, investigate the motion of asteroids in the vicinity of larger bodies, and study the dynamics of binary star systems, among other applications. Although the Hill restricted three-body problem provides an approximation of the real-world scenario, it offers valuable insights into the complex interactions between multiple celestial bodies. The aim of this paper is to explore the Hill three body problem using techniques such as numerical simulations and analytical methods. Specifically, we will study and try to recreate some of the characteristics of the system such as the equation of motion, manifolds, and zero velocity curves. Most importantly, we will study some special solutions and implement methods we learned throughout this quarter to analyze the aforementioned special solutions.

II. Technical Statement Of The Problem

In an inertial frame, the equations of motion for the third body of the restricted 3-body problem can be stated as

$$\ddot{\mathbf{r}} = -\frac{Gm_1}{|\mathbf{r} - \mathbf{r}_1|^3}(\mathbf{r} - \mathbf{r}_1) - \frac{Gm_2}{|\mathbf{r} - \mathbf{r}_2|^3}(\mathbf{r} - \mathbf{r}_2) \quad (1)$$

This equation does not change under transformation to the barycentric frame (only the definitions of \mathbf{r}_1 and \mathbf{r}_2 are different).

*Masters Student, Mechanical and Aerospace Engineering, 9500 Gilman Dr, La Jolla, CA 92093

†Masters Student, Mechanical and Aerospace Engineering, 9500 Gilman Dr, La Jolla, CA 92093

‡Masters Student, Mechanical and Aerospace Engineering, 9500 Gilman Dr, La Jolla, CA 92093

Assuming that the underlying 2-body problem is circular, we recast the equation of motion for the third body into a rotating frame of reference, obtaining the equations of motion for the CR3BP:

$$\ddot{x} - 2\omega\dot{y} = \omega^2 x - \frac{Gm_1}{|\mathbf{r} + \nu R\hat{\mathbf{x}}|^3} (x + \nu R) - \frac{Gm_2}{|\mathbf{r} - (1-\nu)R\hat{\mathbf{x}}|^3} (x - (1-\nu)R) \quad (2a)$$

$$\ddot{y} + 2\omega\dot{x} = \omega^2 y - \frac{Gm_1}{|\mathbf{r} + \nu R\hat{\mathbf{x}}|^3} y - \frac{Gm_2}{|\mathbf{r} - (1-\nu)R\hat{\mathbf{x}}|^3} y \quad (2b)$$

$$\ddot{z} = -\frac{Gm_1}{|\mathbf{r} + \nu R\hat{\mathbf{x}}|^3} z - \frac{Gm_2}{|\mathbf{r} - (1-\nu)R\hat{\mathbf{x}}|^3} z \quad (2c)$$

where

$$\omega = \sqrt{\frac{G(m_1 + m_2)}{R^3}} \quad (3)$$

$$\nu = \frac{m_2}{m_1 + m_2} \quad (4)$$

and R is the (constant) distance between masses m_1 and m_2 . We also note that m_2 is taken to be the smaller of the two large masses.

To arrive at the Hill restricted 3-body problem (HR3BP), we move the coordinate system to the location of m_2 , and consider the motion of the spacecraft in the vicinity of the second body. In this frame, we let the position vector be denoted as ρ , related to r in the CR3BP by

$$\mathbf{r} = \boldsymbol{\rho} + (1-\nu)R\hat{\mathbf{x}} \quad (5)$$

We also make the assumptions that $\rho \ll R$ and $m_1 \gg m_2$. Then using the Legendre expansion, we may write the equation of motion for the third body in the HR3BP:

$$\ddot{\rho}_x - 2\omega\dot{\rho}_y = -\frac{Gm_2}{\rho^3}\rho_x + \frac{3Gm_1}{R^3}\rho_x \quad (6a)$$

$$\ddot{\rho}_y + 2\omega\dot{\rho}_x = -\frac{Gm_2}{\rho^3}\rho_y \quad (6b)$$

$$\ddot{\rho}_z = -\frac{Gm_2}{\rho^3}\rho_z + \frac{Gm_1}{R^3}\rho_z \quad (6c)$$

After non-dimensionalizing, the equations are written as:

$$\ddot{\rho}_x - 2\dot{\rho}_y = -\frac{\rho_x}{\rho^3} + 3\rho_x \quad (7a)$$

$$\ddot{\rho}_y + 2\dot{\rho}_x = -\frac{\rho_y}{\rho^3} \quad (7b)$$

$$\ddot{\rho}_z = -\frac{\rho_z}{\rho^3} - \rho_z \quad (7c)$$

Henceforth the components of ρ will simply be written as x , y , and z . Under these equations of motion, the Jacobi integral can be written as

$$J = \frac{1}{2}v^2 - \frac{1}{\rho} - \frac{1}{2}(3x^2 - z^2) \quad (8)$$

The Jacobi integral is constant throughout the orbit since this is a time invariant system.

III. Solution Techniques and Validation

In order to integrate the above equations, the three second-order equations of motion were written as a system of six first-order equations of motion and implemented in MATLAB. The system was then integrated using `ode45` or `ode113` depending on the particular problem.

To demonstrate that the integrator is working as expected, two non-trivial orbits in the Earth-Moon system are plotted below, along with the value of the Jacobian (normalized against the initial value at $t = 0$ to show conservation). The left trajectory's initial conditions were taken from initial conditions in the CR3BP which give a stable, periodic

butterfly orbit; under the HR3BP dynamics, this orbit is not observed, but still somewhat resembles a butterfly orbit. Stable, periodic orbits in the HR3BP system are discussed later. The right trajectory is simply a nearly-circular orbit.

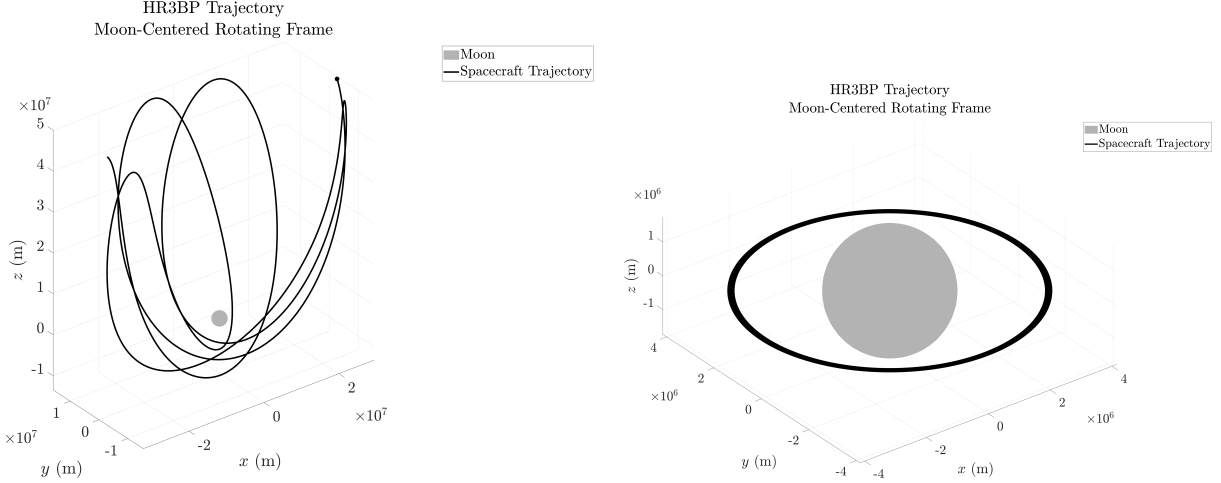


Fig. 1 Sample Orbits in Rotating Frame

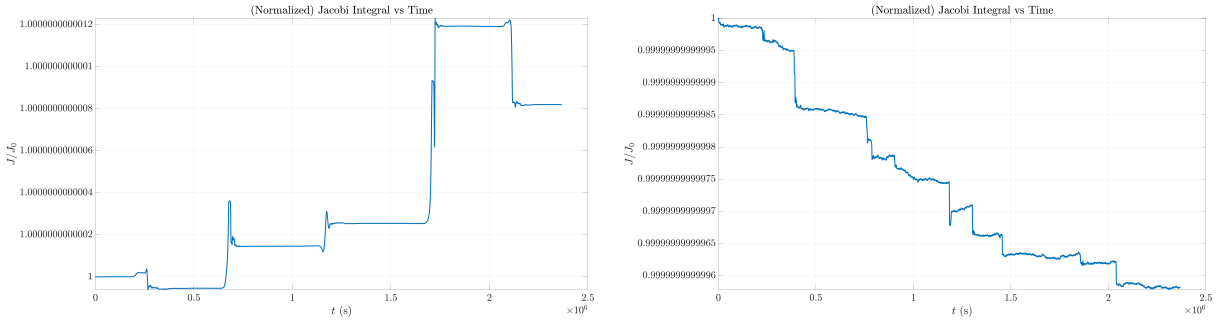


Fig. 2 Jacobi Integrals for Above Orbits

The above orbits were also plotted in an inertial frame to visualize their trajectories relative to the Earth.

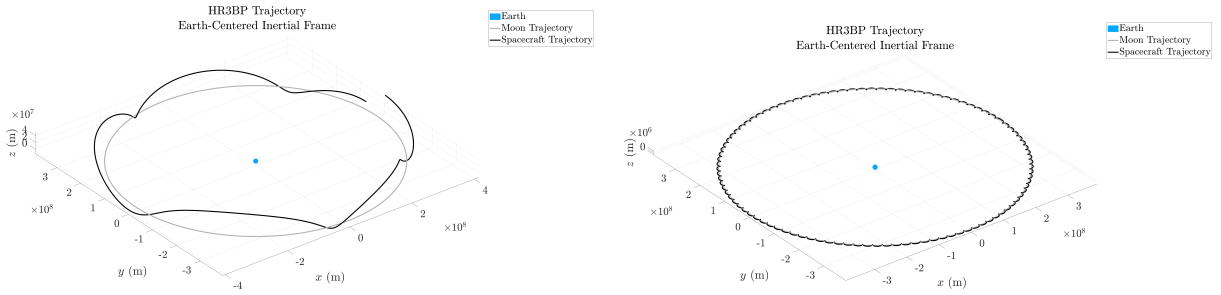


Fig. 3 Sample Orbits in Inertial Frame

Based on the results shown in Figure 2, it is clear that our integrators conserve the Jacobi constant. We conclude that our integrator is working as expected and accurate.

IV. Problems Analyzed

A. Stable and Unstable Manifolds about the L2 Equilibrium Point

One important study that can be carried out in the HR3BP is the determination of the stable and unstable manifolds that allow the transfer to or from the equilibrium points. The equilibrium points L1 and L2 that we will be focusing on more closely are located at $L_2 = (\left(\frac{1}{3}\right)^{\frac{1}{3}}, 0, 0)$ and $L_1 = (\left(-\frac{1}{3}\right)^{\frac{1}{3}}, 0, 0)$. This is simplified by the determination of the eigenvalues and eigenvectors of the dynamic system at the equilibrium points.

To solve the eigenvalues and eigenvectors at these points we need to compute the linearized equations of motion. The linear equations about these equilibrium points is

$$\delta \ddot{r} + 2 \begin{bmatrix} 0 & -1 & 0 \\ 1 & 0 & 0 \\ 0 & 0 & 0 \end{bmatrix} \delta \dot{r} = \begin{bmatrix} 9 & 0 & 0 \\ 0 & -3 & 0 \\ 0 & 0 & -4 \end{bmatrix} \delta r \quad (9)$$

with an associated characteristic equation of,

$$(\lambda^2 + 4)(\lambda^4 - 2\lambda^2 - 27) = 0 \quad (10)$$

The eigenvalues associated with the stable/unstable manifolds about L2 are $\lambda = \pm 2.508$. Solving for the eigenvectors associated with these eigenvalues by analyzing the Hamiltonian Dynamic system of equations, we can perturb the state vector at the L2 equilibrium in the direction of the stable/unstable eigenvectors. We can thus propagate forward in time to visualize the unstable manifold and backward in time to visualize the stable manifold. The plot below shows these trajectories as well as the forbidden region. The forbidden region will be described in detail in the following section.

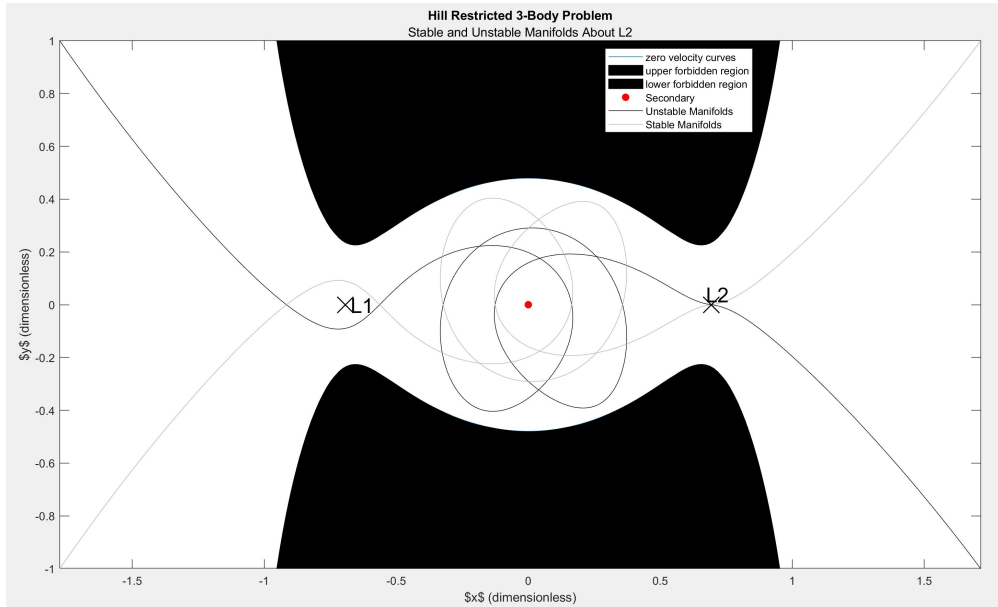


Fig. 4 Stable and Unstable Manifolds

B. Zero-velocity Curves and Surfaces

Another area of focus is the zero velocity curves and surfaces. In order to analyze these curves we must first assume that in Eq.(7) the velocity is 0. Furthermore, since we are looking for the curves and not the surfaces, we will assume the z components to be 0 and solve this implicit function to find the values of x and y. To visualize the planar effects from the zero velocity you would leave the z component and solve the implicit function in a similar manner.

In order to validate our manifolds, trajectories, and zero velocity surfaces, we referenced [1]. We were able to match our eigenvalues and eigenvectors for our manifolds to be the same, as well as the zero velocity curves. Moreover, we confirmed the phenomenon of trajectories "hitting" the zero velocity wall with [1].

The zero velocity surfaces and curves serve as critical boundaries that delineate the permissible regions through which an orbit can traverse. They play a fundamental role in characterizing the dynamics of the three-body system. An important criterion for spacecraft motion within these regions is the value of the Jacobi constant. When the Jacobi constant is equal to or greater than zero, the third body has no restriction to where it can go within the system. However, if the Jacobi constant takes on a negative value, it imposes a significant constraint manifested by the zero velocity surface. This surface acts as an impassable barrier for trajectories approaching it, resulting in a rebound-like effect upon impact with its "walls." The insufficient energy within the system prevents the trajectory from breaking through the surface. In some scenarios, the Jacobi constant can be so negative that it can't leave from either the primary or secondary orbit. One note to add is that the more negative the Jacobi constant is, the larger the barrier until there is no escape. This is shown in Fig[5] and Fig[6].

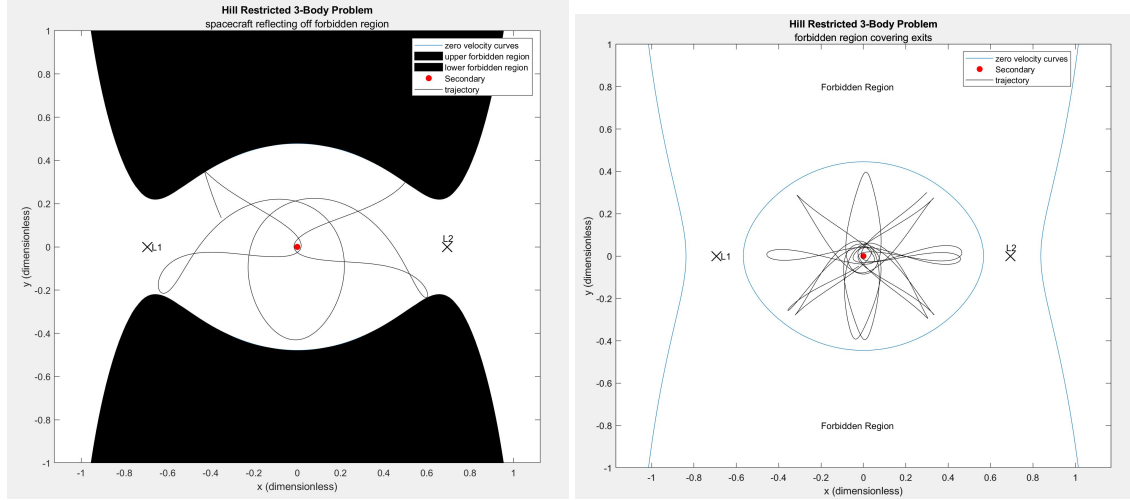


Fig. 5 2D special trajectories on zero velocity curve

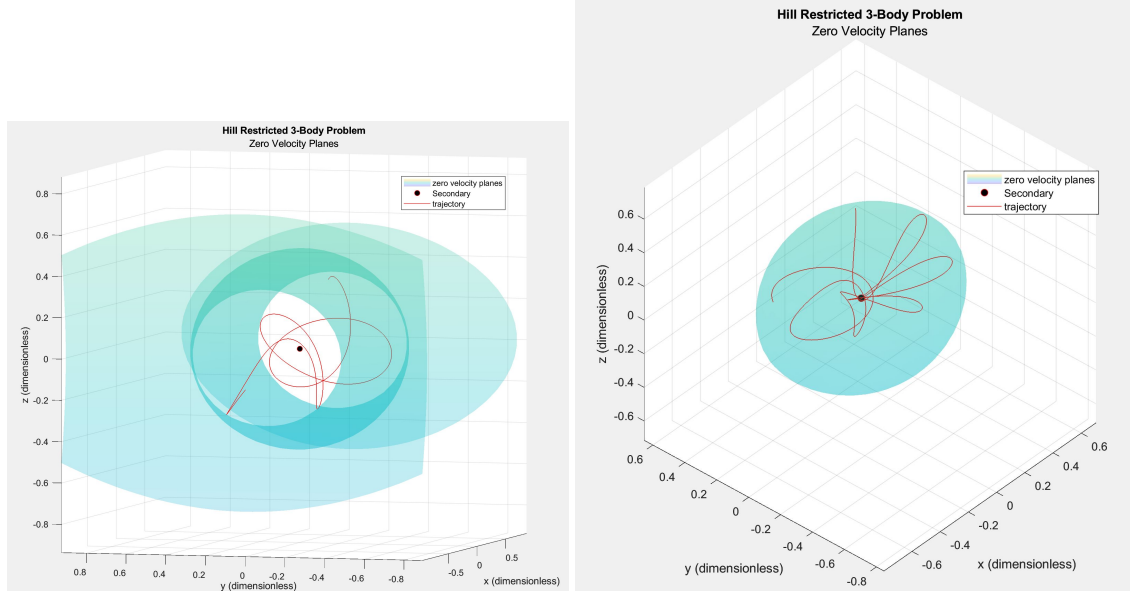


Fig. 6 3D special trajectories on zero velocity curve

C. Periodic orbits for the HRTBP

In any system, the determination of stable, periodic orbits is important; these orbits can be used by satellites to maintain their position near to a body without expending fuel, and certain periodic orbits can be used to aid in the collection of scientific data on the surface from orbit [2]. These orbits are often studied in the context of the HRTBP since many orbits of interest occur very near to the secondary body where the Hill approximation holds. Reference [3] gives the initial conditions for several families of planar orbits in the HRTBP. Some of these families are stable, and some are unstable. One such stable family is plotted in the figure below.

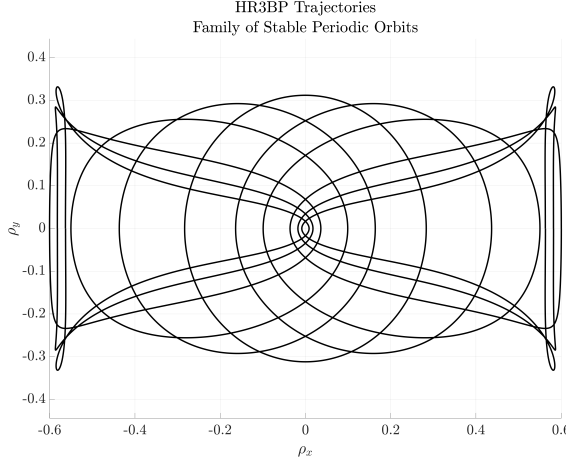


Fig. 7 Family of stable, periodic orbits

These orbits proceed in the counter-clockwise direction (prograde relative to the primary body), and are thus referred to as the low-prograde family of orbits (as opposed to the distant-prograde orbits which are unstable). These orbits can be verified to be stable using the methods described later in this report, but their stability can be (non-rigorously) verified qualitatively by integrating their trajectory for many periods. In the figure above, each orbit was integrated for greater than 10 periods without noticeable deviation from its trajectory.

D. Poincare surface of section

To show that the initial conditions obtained in [3] do indeed produce a periodic orbit, Poincare' surface of section can be employed.

For a set of planar initial conditions, a Poincare section can be defined when $y = 0$ and $\dot{y} < 0$. By implementing a simple event function in the existing HRTBP integrator, the time and position when the spacecraft crosses the Poincare section can be recorded.

Fig[7] shows the Poincare surface of section for a set of initial conditions where the x_0 position is 0.2835 and the Jacobi constant is 4.4999. Clearly, from the elliptical shape of the figure and the minute scale of the x axis, it can be seen that for this set of initial condition, the orbit does exhibit property of periodicity.

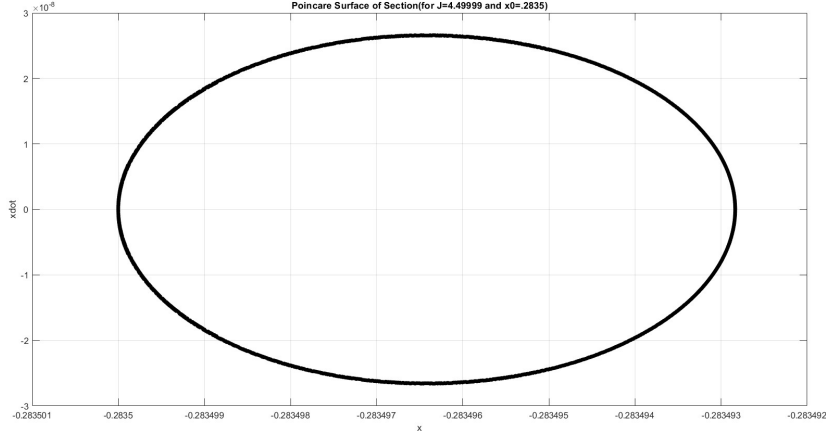


Fig. 8 Poincare surface of section for a periodic orbit

Fig[8] below shows a Poincare surface of section generated from initial conditions near the L2 point with slight perturbations in the state vector. In stark contrast with Fig[7], instead of a clear elliptical pattern, Fig[8] produces a sea of chaotic behaviors that shows no apparent signs of periodic property.

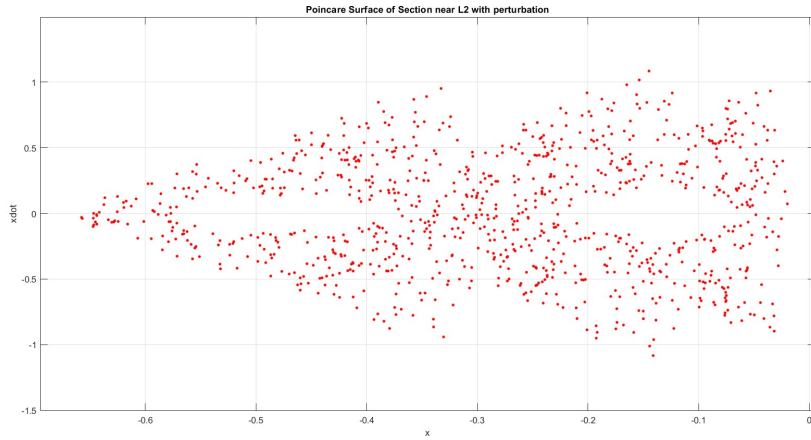


Fig. 9 Poincare surface of section for a chaotic, non periodic orbit

E. Stability analysis-Lyapunov Characteristic Exponent

We can study the stability of these periodic orbits by computing the Lyapunov Characteristic Exponent(LCE). The main idea is that if a trajectory in a Hamiltonian dynamical system is unstable, it means neighboring trajectory will diverge exponentially. On the other hand, if it's stable, then neighboring trajectories will remain close or leave slower than exponentially.

The LCE is defined as χ and is computed using the below equation, where $\Delta x(t)$ is the deviation of the state vector of the two trajectories at time t and Δx_0 is the initial deviation.

$$\chi_t = \frac{1}{T} \ln \left[\frac{\Delta x(t)}{\Delta x_0} \right] \quad (11)$$

After obtaining χ , the stability of the periodic orbit is then determined by the following:

$$\lim_{t \rightarrow \infty} \chi_t \begin{cases} \neq 0, \text{unstable} \\ = 0, \text{stable} \end{cases} \quad (12)$$

For an infinite time period, χ would approach zero if the orbit is stable and would deviate from zero if it's unstable

Using the same initial conditions that were used to plot the Poincare surface of section, we can show that the periodic orbit is indeed stable, as indicated in [3]. Fig[10] below shows the computed LCE value over a period of [0 10] non-dimensional time.

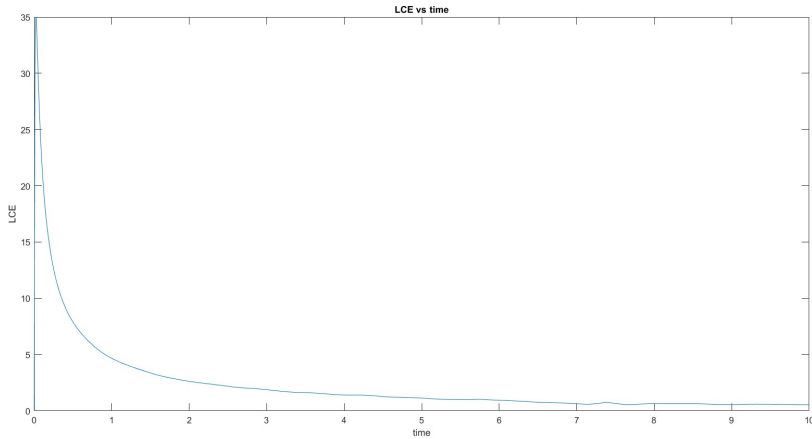


Fig. 10 Time evolution of LCE of a periodic orbit

The LCE converges to zero as indicated above, showing that the periodic orbit is stable.

V. Discussion

From Fig[4] we can see how the stable and unstable manifolds react around the secondary body to then escape. An important thing to note is that going from L2 past the secondary body and through L1, you will go into a much larger Jacobi zero velocity curve that wraps around the primary. This curve delineates a region where spacecraft can achieve a zero relative velocity relative to the rotating frame of the three-body system. This allows us to use the stable and unstable manifolds as a means to seamlessly navigate around celestial bodies that meet the Hill criteria. Notably, this can be accomplished without expending additional energy.

Fig[5] and Fig[6] present compelling visualizations showcasing the fascinating dynamics of spacecraft interacting with the zero velocity curves. These plots on the left of both plots depict the consequences of reaching the boundaries, often referred to as "walls," of these curves. They exemplify how a spacecraft would bounce off the wall and go back into orbit. Furthermore, the plots in Fig[5] and Fig[6] on the right show when a spacecraft finds itself ensnared within the confines of the zero velocity curve where it can't get out of the grasp of the primary or secondary body. Its only viable course of action would involve the application of thrust or the utilization of an external energy source capable of propelling it out of the zero velocity surface.

Figure 7 shows a family of stable, periodic, planar orbits in the HRTBP. These orbits could be used by a satellite to remain indefinitely in the orbit of a secondary body without expending fuel; because the orbits are stable, they are resistant to perturbation, for example from distant bodies or gravitational irregularities of the secondary. Initially, we had hoped to depict a family of stable halo orbits about the L2 Lagrange point; however, it proved difficult to find a reference which would provide the required initial conditions. In the future, a periodic orbit finder could be implemented to find arbitrary periodic orbits via a shooting method.

The Poincare surface of section is a useful tool to understand the dynamics of a system, especially for a high-dimensional one. It reduces the dimensions and offer insights into aspects including stability, periodicity and bifurcation of orbits. The usefulness of the Poincare surface of section can be clearly seen From Fig[8] and Fig[9], allowing us to determine the periodicity almost instantly. For periodic orbits, the Poincare surface of section would exhibit a strong, discernible shape or pattern where as for non-periodic orbits, it would exhibit chaotic behaviors.

In addition to finding the Lyapunov characteristic exponent, other stability analysis methods such as the Floquet theory can be implemented. By applying it, small evolution of perturbations can be investigated to determine whether a periodic orbit is stable or unstable. To apply the Floquet theory, the system would first have to be linearized by calculating the Jacobian matrix of the equations of motion with respect to state variables. The monodromy matrix would later have to be computed in order to find the eigenvalues, which determines the stability of the system.

Due to previous mistakes, we incorrectly showed that the periodic orbit is unstable during our presentation, which contradicts the data given in [3]. After debugging the LCE code, we were able to correct it.

VI. conclusion

In conclusion, the Hill Restricted Three Body Problem presents a captivating framework for studying the dynamics of a spacecraft within a three-body system: stable and unstable manifolds, zero velocity curves, periodic orbits, and Poincare maps are all easily studied in the context of the HR3BP. We studied motion near the L1 and L2 Lagrange points which can be analyzed in order to make use of their dynamics for orbital maneuvers and potential escapes. We showed examples of periodic orbits which can be determined and utilized for science missions, keeping satellites in stable orbits without the need to expend fuel. We also computed Poincare maps and LCE's to show the stability of periodic trajectories. All this and more is possible using the dynamics of the HR3BP: serving as a model problem, it can be utilized to enhance our understanding of celestial mechanics and pave the way for future space exploration missions.

Acknowledgements

We would like to thank Professor Rosengren for providing us with proper references and inspiring us to study this problem.

References

- [1] Scheeres, D. J., *Orbital motion in strongly perturbed environments: Applications to asteroid and Comet Orbiters*, Springer, 2014.
- [2] Paskowitz, M. E., and Scheeres, D. J., “Design of science orbits about planetary satellites: Application to Europa,” *Journal of Guidance, Control, and Dynamics*, Vol. 29, No. 5, 2006, pp. 1147–1158. <https://doi.org/10.2514/1.19464>.
- [3] Henon, M., “Numerical exploration of the restricted three-body problem,” *Symposium - International Astronomical Union*, Vol. 25, 1966, pp. 157–169. <https://doi.org/10.1017/s0074180900105431>.
- [4] NASA, “Three-body periodic orbits,” https://ssd.jpl.nasa.gov/tools/periodic_orbits.html, 2023. Accessed: 2023-06-14.
- [5] Russell, R. P., “Global search for planar and three-dimensional periodic orbits near Europa,” *The Journal of the Astronautical Sciences*, Vol. 54, No. 2, 2006, pp. 199–226. <https://doi.org/10.1007/bf03256483>.
- [6] Scheeres, D. J., Guman, M. D., and Villac, B. F., “Stability Analysis of planetary satellite orbiters: Application to the Europa Orbiter,” *Journal of Guidance, Control, and Dynamics*, Vol. 24, No. 4, 2001, pp. 778–787. <https://doi.org/10.2514/2.4778>.
- [7] Vallado, D. A., and McClain, W. D., *Fundamentals of astrodynamics and applications*, Microcosm Press, 2007.